

Symmetry-induced gap opening in graphene superlattices

Rocco Martinazzo, Simone Casolo and Gian Franco Tantardini

*Department of Physical Chemistry and Electrochemistry,
University of Milan, V. Golgi 19, 20133 Milan, Italy and*

*CIMAINA, Interdisciplinary Center of Nanostructured Materials and Interfaces,
University of Milan. E-mail: rocco.martinazzo@unimi.it*

We study $n \times n$ honeycomb superlattices of defects in graphene. The considered defects are missing p_z orbitals and can be realized by either introducing C atom vacancies or chemically binding simple atomic species at the given sites. Using symmetry arguments we show how it is possible to open a gap when $n = 3m + 1, 3m + 2$ (m integer), and estimate its value to have an approximate square-root dependence on the defect concentration $x = 1/n^2$. Tight-binding calculations confirm these findings and show that the induced-gaps can be quite large, e.g. ~ 100 meV for $x \sim 10^{-3}$. Gradient-corrected density functional theory calculations on a number of superlattices made by H atoms adsorbed on graphene are in good agreement with tight-binding results, thereby suggesting that the proposed structures may be used in practice to open a gap in graphene.

The recent fabrication of graphene[1], a one atom-thick layer of carbon atoms arranged in a honeycomb lattice, has triggered a wealth of studies in both fundamental and applied science. Graphene is a zero-gap semiconductor with a linear dispersion at the Fermi level in which low-energy excitations mimic the behaviour of relativistic massless fermions[2, 3] (see [4, 5] for reviews). This gives rise to a number of interesting phenomena such as an anomalous quantum Hall effect[2, 3] and quasirelativistic Klein tunneling[6]. Its unconventional transport properties with ballistic transport on submicrometer scale[7] and with carrier mobilities up to $2 \cdot 10^5 \text{ cm}^2 \text{ V}^{-1} \text{ s}^{-1}$ [8] offer the possibility of high-performance interconnects in an hypothetical carbon-based nanoelectronics. However, since conductivity cannot be turned completely off, pristine graphene cannot be used as a transistor in logic applications, where high on/off ratios are required[9, 10]. Field-switching capabilities depend on the presence (and size) of a gap in the electronic structure. Electron confinement can be used to open a gap inversely proportional to the confinement length when rolling up graphene into single-walled nanotubes or cutting its edges to form nanoribbons. Both these possibilities have been exploited, and promising carbon nanotube/nanoribbons field-effect transistors realized[9].

In this Letter we explore a different possibility made available by recent progresses in patterning graphene with lithographic techniques[11, 12]. Specifically, we study $n \times n$ honeycomb superlattices of defects on graphene (defined to be periodic structures of defects arranged to form a honeycomb lattice commensurate with the substrate) and use symmetry arguments to design semiconducting structures. We show that a gap can be opened by preserving graphene symmetry. We estimate that an inverse proportionality to the (super)lattice constant n approximately holds for the gap size in these structures, and use tight-binding and *first-principles* calculations to validate these predictions. The computed gaps are sizable and compare favourably with those found in nanoribbons at the same length scale[13]. In the following we first present our symmetry arguments and derive general rules to open a gap in the considered

superlattices. We then estimate its value and present the results of numerical calculations.

Graphene's unconventional electronic properties are strictly related to its D_{6h} point symmetry. The k -group at the K (K') high-symmetry points (D_{3h}) allows for doubly degenerate irreducible representations, and Bloch functions built with p_z orbitals of the A and B sublattices span one of its two-dimensional irreducible representation (irrep), namely E'' . This is enough for the $\pi - \pi^*$ degeneracy at the K (K') point and for the unusual linear dispersion relation, irrespective of the level of approximation[14]. These properties are captured by the simple tight-binding (TB) model Hamiltonian

$$H = -t \sum_{\langle i,j \rangle} a_i^\dagger b_j + H.c. - t' \sum_{\langle\langle i,j \rangle\rangle} a_i^\dagger a_j - t' \sum_{\langle\langle i,j \rangle\rangle} b_i^\dagger b_j \quad (1)$$

where a_i^\dagger (b_i^\dagger) is the creation operator for an electron on site i of the A (B) sublattice, the first sums run over nearest neighboring sites in the honeycomb lattice and the second sums run over sites which are nearest neighbors in the triangular sublattices. The hopping t has been estimated to be ~ 2.7 eV whereas $t' \ll t$ has different values depending on the parametrization. When $t' = 0$ the Hamiltonian describes a bipartite system, and we assume that this approximately holds for graphene. The consequences of relaxing this approximation will be addressed numerically at the end of this Letter.

Bipartitism has a large impact on the electronic structure *via* the induced electron-hole symmetry. For instance, it has long been known that in bipartite systems, at half filling, sublattice imbalances due to vacancies strongly affect the energy spectrum at the Fermi level through the introduction of midgap states[15]. In graphene, such states have a semidelocalized nature with a $1/r$ dependence on the distance from the defect[16]. By introducing an equal number of defects on each sublattice one restores balance, eliminates midgap states and a gap possibly opens. In general, however, there is no guarantee that the gap opens at K and does not close somewhere else in the Brillouin zone (BZ). Therefore, we focus here on $n \times n$ honeycomb pat-

terns of defects only, in such a way to constrain (by symmetry) the changes in the band structure and possibly reduce accidental degeneracies. In these structures the high-symmetry points where degeneracy is expected are the Γ and K points, that is where the k -groups (D_{6h} and D_{3h} , respectively) allow for doubly degenerate irreps. In the following we use E (A) for a generic two- (one-) dimensional irreducible representation, and denote as K_n the K point of the nxn superlattice BZ (SBZ). For a strictly bipartite system at half-filling, degeneracy at the Fermi level occurs when the number of E irreps is odd; when this number is even degeneracy, if occurs, can be considered as accidental. Therefore, introducing symmetric defects in such a way to have an even number of E irreps *both* at the Γ and at the K point a gap generally opens.

To show that this is indeed possible, we consider a generic nxn supercell and count the number of A and E irreps generated by the carbon atoms in cell (the so-called atomic representations). To this end, it is sufficient to consider that half of the cell which has D_{3h} symmetry with respect to its center I (see Fig. 1), the remaining half behaving similarly. These two half-cells (α and β in the following) play the role of A and B type of sites in the honeycomb superlattice. In each of them, the set of C atoms may be grouped in classes of equilateral triangles $\Delta_{i,\alpha}$ ($\Delta_{i,\beta}$), plus a possible atom at I_α (I_β) as it happens when $n = 3m + 1$ and $n = 3m + 2$ (m integer). Each triangle spans an $A + E$ irrep of the D_{3h} group (centered at I) which behave as s and (p_x, p_y) orbitals centered at I ; the atom at I , when present, spans of course an A irrep. Then, by considering Bloch functions built with these s - and (p_x, p_y) - like orbitals it is possible to count the number of A and E irreps for each case. At Γ the Bloch functions built with s -like orbitals centered on I_α and I_β span two A representations, whereas p_x, p_y -like functions span two E irreps; at K_n the first generate an E irrep whereas the latter span $2A + E$. These are also the irreps generated by the p_z orbitals of the C atoms as long as we discriminate between A and E type only. The overall result is given in Table I where the symbol $\bar{n}_3 = \bar{0}_3, \bar{1}_3, \bar{2}_3$ identifies the three (congruence) classes modulo 3, i.e. the sequences $n = 3m, 3m + 1$ and $3m + 2$, respectively.

It follows from Table I that with the full atomic set (i.e. considering pure graphene) degeneracy occurs at the K_n points when either $n \in \bar{1}_3$ or $n \in \bar{2}_3$. This is consistent with the folding $K(K') \rightarrow K_n(K'_n)$ and $K(K') \rightarrow K'_n(K_n)$, respectively. In the case $n \in \bar{0}_3$ both K and K' folds to Γ and therefore a 4-fold degeneracy occurs; this can be considered accidental in this context as it cannot be predicted by the number of E irreps only. More interestingly, two important results concerning the introduction of p_z -vacancies are easily proved.

I. *By removing a $\Delta_{i,\alpha}, \Delta_{i,\beta}$ pair only is not generally possible to open a gap.* Here, $2(A + E)$ irreps are removed both at Γ and at K_n , and no modification occurs on the parity of the E sets. Exceptions to this rule are,

Γ	A	E
$\bar{0}_3$	$2n^2$	$2n^2$
$\bar{1}_3$	$2(3n^2 + 2n + 1)$	$2(3n^2 + 2n)$
$\bar{2}_3$	$2(3n^2 + 4n + 2)$	$2(3n^2 + 4n + 1)$
K_n	A	E
$\bar{0}_3$	$2n^2$	$2n^2$
$\bar{1}_3$	$2n(3n + 2)$	$2n(3n + 2) + 1$
$\bar{2}_3$	$2(3n^2 + 4n + 1)$	$2(3n^2 + 4n + 1) + 1$

Table I: Number of irreducible one- (A) and two- (E) dimensional representations (per cell) generated by the full atomic basis on a nxn honeycomb superlattice at the Γ and K points of the corresponding BZ.

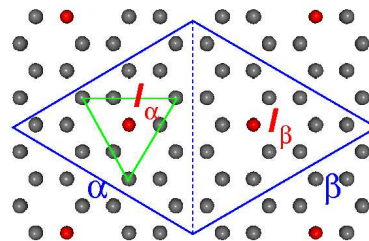


Figure 1: The simplest symmetrically defective superlattice for $n = 4$. Also indicated the two halves of the cell (α, β), their centers I_α, I_β (red balls) and a triangle $\Delta_{i,\alpha}$. A defect is a missing p_z orbital at I_α, I_β .

of course, those cases where degeneracy is accidental (as pure graphene in the $\bar{0}_3$ case which does show a gap after removal of one such pairs, see below).

II. *When $n \in \bar{1}_3$ or $n \in \bar{2}_3$ removal of the atoms at I_α and I_β does open a gap.* In these cases, the atomic basis spans $2A$ at Γ and E at K_n , thereby turning the number of E irreps to be even at *both* special points. Also in this case, exceptions of residual accidental degeneracy are possible.

The second result provides a very simple way for opening a gap in two thirds of the cases, that is by introducing a p_z vacancy at I_α and I_β . In practice, this can be realized by either removing substrate atoms or using them to covalently bind simple adsorbates such as H atoms[17]. In the latter case, indeed, the C atoms involved in the chemisorption process turn their hybridization to sp^3 and effectively get out of the $\pi - \pi^*$ band system. In this Letter we focus on the simplest defective superlattices, i.e. those with vacancies at I_α and I_β *only*, and call them $(n, 0)$ -honeycombs. In general, the pair of integers (n, p) ($p = 0, \dots, \text{int}(n^2/3)$) can be used to identify a nxn honeycomb superlattice with $2p$ equilateral triangles symmetrically removed from the unit supercell, in addition to the atoms at their centers I_α and I_β when $n \in \bar{1}_3 \cup \bar{2}_3$. Fig. 1 shows an example, the $(4, 0)$ -honeycomb.

It is possible to estimate the size of the induced gap at the K_n point of these $(n, 0)$ -honeycombs. To this end, we perform a lattice renormalization[18] by making use of the

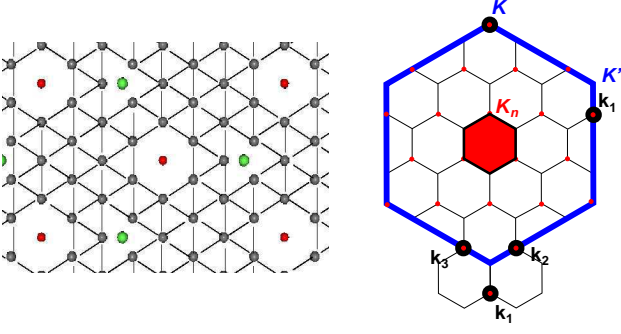


Figure 2: Left panel: the renormalized triangular lattice corresponding to the (4,0)-honeycomb (grey balls). Red and green balls mark the position of the A and B defects. Right panel: Brillouin zones for graphene (blue borders) and for the structure shown on the left panel (red). Also indicated the four lowest-energy \mathbf{k} points (K and \mathbf{k}_i $i = 1 - 3$) for the calculation in the text (black circles).

bipartite nature of the Hamiltonian $H = H_{AB} + H_{BA}$. This simplifies the problem by halving the state space of interest. Indeed, since H only allows transitions from the A to the B subspaces (H_{BA}) and *vice versa* (H_{AB}) it is sufficient to consider the problem in the A space only with Hamiltonian[19] $\tilde{H}_{AA} = H_{AB}H_{BA}$. For any non-zero eigenvalue $\tilde{\epsilon}_i$ and eigenvector $|\psi_{A,i}\rangle$ of this Hamiltonian there exist two solutions of the original problem with eigenvalues $\epsilon_i = \pm\sqrt{\tilde{\epsilon}_i}$ and eigenvectors $|\psi_{A,i}\rangle \pm |\psi_{B,i}\rangle$, where $|\psi_{B,i}\rangle$ is defined to be $|\psi_{B,i}\rangle = \tilde{\epsilon}_i^{-1/2}H_{BA}|\psi_{A,i}\rangle$; if $\tilde{\epsilon}_i = 0$, $|\psi_{A,i}\rangle$ is already a H eigenvector. The converse is also true, namely from any eigenvector $|\psi_i\rangle$ the two projections $|\psi_{A,i}\rangle$ and $|\psi_{B,i}\rangle$ onto the A and B subspaces satisfy $H_{BA}|\psi_{A,i}\rangle = \epsilon_i|\psi_{B,i}\rangle$ and $\tilde{H}_{AA}|\psi_{A,i}\rangle = \epsilon_i^2|\psi_{A,i}\rangle$; that is, in studying \tilde{H}_{AA} one only misses possible zero eigenstates in the B subspace[20]. In graphene the renormalized Hamiltonian \tilde{H}_{AA} describes a triangular lattice with on-site energy t^2Z (where t is the hopping term of eq.1 and $Z = 3$ is the coordination number of A atoms in the original honeycomb lattice) and hopping t^2 between neighbors in the triangular lattice. Defects are of two kinds: while A vacancies translate simply into A vacancies in the renormalized lattice, B vacancies modify both the coordination number and the hopping between A sites. The renormalized $(n,0)$ -honeycomb for $n = 4$ is shown in the left panel of Fig.2, whereas the right panel of the same figure displays its SBZ along with the graphene BZ. The state space at K_n is given by its n^2 replicas within BZ and comprises K or K' depending on whether $n \in \bar{1}_3$ or $n \in \bar{2}_3$. Quasi-degenerate perturbation theory is necessary to estimate the ground-state energy $\tilde{\epsilon}_0(K_n)$ (and hence the gap $\epsilon_{gap} = 2\sqrt{\tilde{\epsilon}_0}$), but it becomes intractable at large n (i.e. at very small defect concentration $x = 1/n^2$) because a huge number of K_n replicas gets close to the K and K' points. Therefore, we consider x sufficiently small that the defects are isolated from each other, but large enough that a few state calculation is reliable. The smallest set of K_n replicas contains K and the

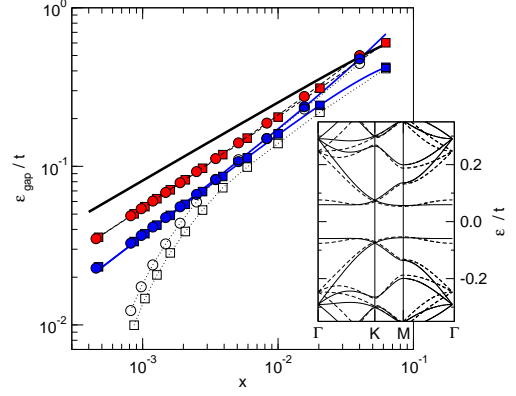


Figure 3: Energy gaps (in units of t) for the $(n,0)$ -honeycombs as functions of $x = 1/n^2$. Bold black line is the gap at K_n as estimated using Eq. 3. Filled symbols are for results of tight-binding calculations with $t' = 0$ and bold blue lines are best-fit curves (see text): squares for $n \in \bar{1}_3$, circles for $n \in \bar{2}_3$; red symbols for the gap at K_n , blue for the full gap. Open symbols are full gap results for $t' = 0.1t$. The inset shows the low-energy band structures of the (13,0) (solid lines) and (14,0) (dashed lines) honeycombs as obtained from tight-binding calculations with $t' = 0$.

\mathbf{k}_i vectors ($i = 1 - 3$) shown in Fig.2 (right panel) for the case $n = 4$, and corresponds to the set of Bloch functions $|\psi_0\rangle = |\psi_K\rangle$ and $|\psi_i\rangle = |\psi_{\mathbf{k}_i}\rangle$ built with p_z orbitals at A sites; the case $n \in \bar{2}_3$ is analogous except that K is replaced with K' . $|\psi_0\rangle$ spans the A_2'' irrep of the k -group at K_n (D_{3h}), whereas $\{|\psi_i\rangle\}$ span $A_2'' + E''$. Thus it is possible to set up a two dimensional problem in the A_2'' subspace. The corresponding Hamiltonian matrix can be obtained from the \tilde{H}_{AA} matrix elements between (graphene) Bloch states, Eq.2

$$\begin{aligned} \langle \psi_{\mathbf{k}'} | \tilde{H}_{AA} | \psi_{\mathbf{k}} \rangle &= t^2 \delta_{\mathbf{k},\mathbf{k}'} (3 + F(\mathbf{k})) \\ &\quad - xt^2 \delta_{\mathbf{k},\mathbf{k}'+\mathbf{g}} \left\{ e^{ig\delta_A} (3 + F(\mathbf{k}') + F(\mathbf{k})) \right. \\ &\quad \left. + e^{ig\delta_B} f(\mathbf{k}')^* f(\mathbf{k}) \right\} \end{aligned} \quad (2)$$

Here $F(\mathbf{k}) = \sum_{i=1}^6 e^{-i\mathbf{k}\delta'_i}$, $f(\mathbf{k}) = \sum_{i=1}^3 e^{-i\mathbf{k}\delta_i}$ (where δ'_i and δ_i are the vectors joining AA and AB nearest-neighbors, respectively), \mathbf{g} is a reciprocal superlattice vector and δ_A, δ_B are the position vectors of the defects in the unit supercell. In deriving Eq. 2 periodicity of the superlattice has been used and the defects have been considered as isolated ($n > 2$). With the help of Eq. 2 and of the symmetry properties of $F(\mathbf{k})$ and $f(\mathbf{k})$, the Hamiltonian matrix in the above A_2'' space reads as

$$t^2 \begin{bmatrix} 3x & -x\sqrt{3}F_x \\ -x\sqrt{3}F_x & 3 + F_x - 9x(2 + F_x) \end{bmatrix} \quad (3)$$

where $F_x = F(\mathbf{k}_1) \sim -3 + 3(2\pi/3)^2x - \sqrt{3}(2\pi/3)^3x^{3/2}$. The lowest eigenvalue $\tilde{\epsilon}_0 (\sim 3xt^2(0.561 - 0.961\sqrt{x}))$ allows us to estimate the energy gap ϵ_{gap} at the K_n point.

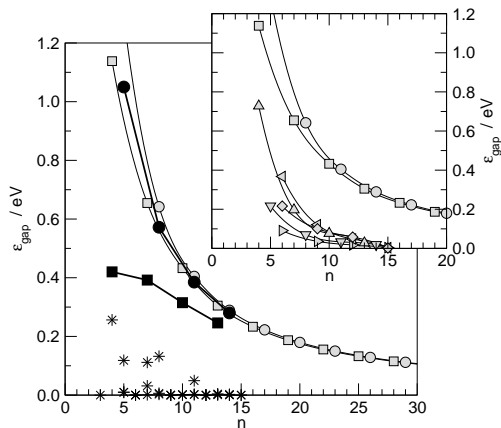


Figure 4: DFT results for the energy gap in $(n,0)$ -honeycombs made by adsorbed H atoms as functions of n (filled symbols). For comparison, also reported are the tight-binding results of Fig. 3 (open symbols) with $t = 2.7$ eV and $t' = 0$. Squares for $n \in \bar{1}_3$, circles for $n \in \bar{2}_3$. Stars are energy gaps in a number of superlattices with an asymmetric AB pair of defects per cell (*ortho*- and *para*- dimers *not* included). The inset shows TB results (normalized to the number of pairs of defects) for a number of (n,p) honeycombs: triangles for $p = 1$, diamonds for $p = 2$. (Lines are guide to eyes).

This is plotted in Fig.3 as a function of x along with the results of tight-binding calculations. The importance of including a larger number of K_n replicas close to (K, K') is evident at small x where the energy gap decreases slightly faster than \sqrt{x} ; the best-fit to the numerical results gives an exponent ~ 0.66 . Tight-binding calculations reveal that the minimum gaps occurs either at M or Γ (see inset of Fig.3), depending on x and on the sequence considered, but behave similarly to the gaps at K_n . Differences between the two sequences appear at large x and reflects the different shape of the low-energy bands (not shown). A best-fit of $\varepsilon_{gap} = ax^\alpha(1 + bx^\beta)$ to the numerical results, also reported in Fig.3, gives $(a, b, \alpha, \beta) = (3.34, -4.99, 0.65, 1.14)$ for $n \in \bar{1}_3$ and $(3.37, +2.9, 0.66, 0.88)$ for $n \in \bar{2}_3$. We have also investigated the effect of breaking the electron-hole symmetry by performing tight-binding calculations with $t' \neq 0$. Introduction of the next-to-nearest neighbors interaction only affects the results at small x , where the valence and conduction bands start to overlap at some point x_c because of the asymmetry introduced in the energy spectrum. The position of this critical value x_c shifts to larger x when increasing t' but remains small for realistic values (for $t' = 0.1t$ used in Fig.3 $x_c < 10^{-3}$). Notice that the effect of next-to-nearest neighbor interactions is different for the two sequences considered.

To further investigate this point and, more importantly, to address the role of electron correlation we performed gradient-corrected density-functional-theory (DFT) calculations on a number of $(n,0)$ -honeycombs of adsorbed H atoms. The details of the calculations are analogous to those reported in a previous work[17], except for the fact

that a finer mesh of \mathbf{k} points has been used to correctly compute the energy gaps. The results are reported in Fig.4 up to $n = 14$ ($x \sim 0.005$); for larger values of n DFT calculations become prohibitive. As can be seen from Fig. 4 DFT results show a reduced gap size with respect to TB ones in all the cases considered but the effect is much more pronounced in the $\bar{1}_3$ sequence than in the $\bar{2}_3$ one. In particular, DFT results for $n = 5, 8, 11, 14$ closely parallel the TB ones (t has been set to its accepted value, $t = 2.7$ eV), despite the fact that the first refer to a realistic situation where defects are H atoms while in TB calculations defects are modeled by simple p_z vacancies. Discrepancies in the $\bar{1}_3$ sequence at small n needs further investigation, though it is in line with the introduction of the next-to-nearest neighbor hopping (Fig. 3). Similar behaviour was found for the gap in armchair graphene nanoribbons where it was explained by the modified nearest-neighbor hoppings for the sites close to the defect[13]. In any case, both the size of the gap and its dependence on n are promising for future applications.

Finally, to underline the role played by symmetry in designing the defective structures, TB results for different superlattices are also reported in Fig. 4. Notice that the $(n,0)$ honeycombs considered in this Letter show the largest gaps with the minimum number of defects per supercell (see the inset of Fig.4, where the results for a number of (n,p) -honeycombs with $n \in \bar{0}_3$ are also reported).

To summarize, we have studied graphene superlattices of defects where a gap at the Fermi level opens because of symmetry. Tight-binding and density-functional-theory calculations show that the gap is indeed sizable, thereby suggesting that the proposed structures may play a role in designing future carbon-based electronic devices.

-
- [1] K. S. Novoselov, A. K. Geim, S. V. Morozov, D. Jiang, Y. Zhang, S. V. Dubonos, I. V. Gregorieva, and A. A. Firsov, *Science* **306**, 666 (2004).
 - [2] K. S. Novoselov, A. K. Geim, S. V. S. V. Morozov, D. Jiang, M. I. Katsnelson, I. V. Gregorieva, S. V. Dubonos, and A. A. Firsov, *Nature* **438**, 197 (2005).
 - [3] Y. Zhang, Y.-W. Tan, H. L. Stormer, and P. Kim, *Nature* **438**, 201 (2005).
 - [4] A. K. Geim and K. S. Novoselov, *Nat. Mater.* **6**, 183 (2007).
 - [5] A. H. Castro Neto, F. Guinea, N. M. R. Peres, K. S. Novoselov, and A. K. Geim, *Rev. Mod. Phys.* **81**, 109 (2009).
 - [6] M. I. Katsnelson, K. S. Novoselov, and A. K. Geim, *Nature Phys.* **2**, 620 (2006).
 - [7] F. Schedin, A. K. Geim, S. V. Morozov, E. W. Hill, P. Blake, M. I. Katsnelson, and K. S. Novoselov, *Nat. Mater.* **6**, 652 (2007).
 - [8] K. Bolotin, K. Sikes, Z. Jiang, M. Klima, G. Fudenberg, J. Hone, P. Kim, and H. L. Stormer, *Solid State Commun.* **143**, 351 (2008).
 - [9] P. Avouris, Z. Chen, and V. Perbeinos, *Nature Nanotech* **2**, 605 (2007).

- [10] K. Novoselov, *Nat. Mater.* **6**, 720 (2007).
- [11] J. C. Meyer, C. O. Girit, M. F. Crommie, and A. Zettl, *Appl. Phys. Lett.* **92**, 123110 (2008).
- [12] M. D. Fischbein and M. Drndic, *Appl. Phys. Lett.* **93**, 113107 (2008).
- [13] Y. W. Son, M. L. Cohen, and S. G. Louie, *Phys. Rev. Lett.* **97**, 216803 (2006).
- [14] J. C. Slonczewski and P. R. Weiss, *Phys. Rev.* **109**, 272 (1958).
- [15] M. Inui, S. A. Trugman, and E. Abrahams, *Phys. Rev. B* **49**, 3190 (1994).
- [16] V. M. Pereira, F. Guinea, J. Lopes dos Santos, N. Peres, and A. Castro Neto, *Phys. Rev. Lett.* **96**, 036801 (2006).
- [17] S. Casolo, O. M. Løvvik, R. Martinazzo, and G. F. Tantarini, *J. Chem. Phys.* **130**, 054704 (2009).
- [18] G. G. Naumis, *Phys. Rev. B* **76**, 153403 (2007).
- [19] If H is the second quantization version of the Hamiltonian a projection onto the single particle space is implied.
- [20] Their presence can easily be detected by defining A to be the majority species and comparing the number of zero A eigenstates with the sublattices imbalance.